Direct Visualization of the Lateral Structure of Porcine Brain Cerebrosides/POPC Mixtures in Presence and Absence of Cholesterol

Matthias Fidorra,[†] Thomas Heimburg,[‡] and Luis A. Bagatolli[†*]

[†]Membrane Biophysics and Biophotonics group/MEMPHYS, Center for Biomembrane Physics, Department of Biochemistry and Molecular Biology, University of Southern Denmark, 5230 Odense, Denmark; and [‡]Membrane Biophysics Group, Niels Bohr Institute, 2100 Copenhagen, Denmark

ABSTRACT We studied the thermal behavior of membranes composed of mixtures of natural cerebrosides (from porcine brain) and 1-palmitoyl-2-oleoyl-*sn*-glycero-3-phosphocholine (POPC) with and without cholesterol, using differential scanning calorimetry, Fourier transform infrared spectroscopy, and confocal/multiphoton fluorescence microscopy. The POPC/cerebroside mixture display solid ordered/liquid disordered phase coexistence in a broad range of compositions and temperatures in agreement with previous results reported for POPC/(bovine brain)cerebrosides. The observed phase coexistence scenario consists of elongated, micrometer-sized cerebroside-rich solid ordered domains that span the bilayer, embedded in a POPC-rich liquid disordered phase. The data obtained from differential scanning calorimetry and Fourier transform infrared spectroscopy was in line with that obtained in the microscopy experiments for the binary mixture, except at very high cerebroside molar fractions (0.8–0.9) were some differences are observed. Cholesterol incorporation exerts strong changes on the lateral organization of POPC/porcine brain cerebroside membranes. At intermediate cholesterol concentrations (10–25 mol %) the solid ordered/liquid disordered phase coexistence scenario gradually transform to a solid ordered/liquid ordered one. Above 25 mol % of cholesterol two distinct regions with liquid ordered phase character are visualized in the membrane until a single liquid ordered phase forms at 40 mol % cholesterol. The observed cholesterol effect largely differs from that reported for POPC/porcine brain ceramide, reflecting the impact of the sphingolipids polar headgroup on the membrane lateral organization.

INTRODUCTION

Cerebrosides are ceramide-based lipids that are present in the myelin sheath of nerve tissue, skin and kidney tissue and epithelial cells of small intestine and colon (1–5). Chemically, they consist of a ceramide moiety with a single sugar residue (hexose) linked at the 1-hydroxyl position of ceramide (5). The most common classes of cerebrosides are galactosylceramides (Galcer) and glucosylceramides, also including zwitterionic glycosphingolipids.

Galcer are found in nervous tissue, with a higher incidence in the white matter (6). The most predominant constituent of white matter is the myelin sheath of the axons, which comprise ~50% of the white matter. Myelin has an atypical low amount of proteins (~20%) and its main lipid constituents are glycosphingolipids, primarily cerebrosides (7). Myelination seems to be very important for nerve impulse propagation as the velocity of nerve conduction in unmyelinated axons decreases drastically. For instance, Bosio et al. showed that mice deficient in Galcer suffer from whole body tremor and a loss of motor activity (8,9). The Galcer deficient mice lacked the enzyme uridine diphosphate galactose/ceramide galactosyltransferase, that is responsible for GalCer biosynthesis from ceramides. Instead of Galcer, glucosylceramides (Glucer) are present to a high percentage in the myelin membranes of these knockout mice (8,9). Remarkably, the conduction velocity of the sciatic nerve of the Galcer deficient mice dropped to that of unmyelinated axons (8). These kinds of phenomena may be associated with the increase in fluidity, permeability and reduced packing observed in myelin when lack of Galcer is present in this particular membrane (10).

Demyelination process also occurs in globoid cell leukodystrophy (Krabbe disease), an inherited fatal disease. Krabbe disease is caused by mutations in the galactocerebrosidase (GALC) gene, which causes a deficiency of galactosylceramidase (that in turn degrade Galcer and psychosines). The buildup of unmetabolized lipids affects the growth of the nerve's protective myelin sheath and causes severe degeneration of motor skills. In this last case the Galcer and psychosines accumulate in globoid cells resulting in the death of the oligodendroglial cells, the cells that myelinate axons (11–14). GalCer is also known to be overexpressed on the surface of a variety of cancer cells. The last is related with the transcriptional repression of the GALC gene that is responsible for degradation of GalCer to ceramides (15). Because ceramides are reported to be apoptosis activators and cerebrosides are reported to be apoptosis inhibitors, an accumulation of GalCer could be responsible for exuberant cell growth observed in cancer tissue (15). Additionally, GalCer have been reported to be an alternative receptor for a HIV glycoprotein (16,17).

Galcer have been studied in different model membrane systems and show high melting phase transition temperatures (7,18–25). The fact that the phase transition of these lipids are well above the physiological temperature suggests that

Submitted August 4, 2008, and accepted for publication March 31, 2009.

*Correspondence: bagatolli@memphys.sdu.dk

Editor: Enrico Gratton.

0006-3495/09/07/0142/13 $2.00

doi: 10.1016/j.bpj.2009.03.060

presence of this lipid may induce order in biological membranes at physiological temperatures (26). Cerebroside membranes are reported to have strong interbilayer interactions and may interact also laterally by hydrogen bonding (26,27). Additionally, depending on the chain length of the cerebroside lipids vesicular and tubular membrane morphologies were observed (26,28).

Maggio et al. (20) studied bovine brain GalCer/dipalmitoylphosphatidylcholine (DPPC) lipid mixture membranes using DCS and report lipid immiscibility from 0% to 46% mol GalCer. On the other hand, experiments with synthetic palmitoyl cerebroside mixed with DPPC showed complete miscibility of lipids up to 23% palmitoyl-cerebroside membrane content; i.e., at higher cerebroside contents a palmitoyl-cerebroside rich solid ordered phase was observed (29).

The phase diagram of 1-palmitoyl-2-oleoyl-*sn*-glycero-3-phosphocholine (POPC)/GalCer (from bovine brain) mixtures was explored by Curatolo (7). This reported POPC/GalCer phase diagram is characterized for presence of solid ordered/liquid disordered -like phase separation over a broad composition and temperature ranges (7). Blanchette et al. (30) observed lateral phase separation on dilauroylphosphatidylcholine (DLPC)/GalCer giant unilamellar vesicles (GUV) and planar lipid membranes using epifluorescence microscopy and atomic force microscopy (AFM). They reported that in membranes composed of DLPC/GalCer 3:1 mol the observed phase separation scenario is abolished by incorporating 12.5% mol of cholesterol. In membranes composed of DLPC/Galcer 1:1 mol phase separation is no longer observed at a cholesterol concentration of 30% mol (30). In a recent publication, the same laboratory investigated the lateral structure of model membranes composed of phosphatidylcholine (PC) phospholipids, GalCer, and cholesterol (24). In these mixtures the degree of saturation of the PC lipids is changed (by using DLPC; POPC or DOPC) (31). The authors found that by increasing the degree of saturation of the phospholipids, micrometer-sized lipid domains persist in the membranes at higher molar fractions of cholesterol in the mixture (31).

In this study, the lateral behavior of porcine brain cerebroside containing membranes is explored using a particular array of experimental techniques; i.e., differential scanning calorimetry (DSC), Fourier transform infrared (FTIR) spectroscopy, and confocal/multiphoton excitation fluorescence microscopy. POPC, a natural occurring phospholipid is mixed with cerebrosides in different ratios with and without different cholesterol molar fractions. This approach permits establishing a correlation among parameters measured in bulk conditions (DSC, FTIR) and the microscopic scenario observed at the level of single giant liposomes. Additionally, taking into account our previous results on ceramide containing membranes (32) we also discuss the impact of the polar headgroup of these two sphingolipids on the lateral structure of different membranes containing POPC and cholesterol.

MATERIALS AND METHODS

Materials

POPC, 1-palmitoyl-(D31)-2-oleoyl-*sn*-glycero-3-phosphocholine (POPC-d31), porcine brain cerebrosides (pb-cerebrosides), ganglioside G_{M1} (Galβ1-3GalNAcβ1-4(NeuAcα2-3)Galα1-4Glcβ1-1′-Cer from ovine brain), cholesterol, and the fluorescence probe 1-palmitoyl-2-[6-[(7-*nitro*-2-1,3-benzoxadiazol-4-yl)amino]hexanoyl]-*sn*-glycero-3-phosphocholine (NBD-PC) were purchased from Avanti Polar Lipids (Alabaster, AL). G_{M1} is used with the aim to identify sphingolipid enriched areas (see Results). To identify G_{M1} distribution on the membrane, Alexa Fluor 488 labeled cholera toxin subunit B is used. Pb-cerebrosides is a complex mixture of galactosyl cerebrosides with different saturated (49%, being 24:0 and 22:0 the most abundant saturated chain species) and unsaturated (11%, mainly 24:1) chain lengths. Notice that 40% of the chain length components for the pb-cerebroside mixture are not reported by the vendor company (see http://www.avantilipids.com/Natural.asp). The probes 1,1′-dioctadecyl-3,3,3′,3′-tetramethylindocarbocyanine perchlorate (DiI_{C18}), 6-dodecanoyl-2-dimethylaminonaphthalene (LAURDAN), and Alexa Fluor 488 labeled cholera toxin subunit B conjugate were purchased from Invitrogen (Copenhagen, Denmark).

Methods

Preparation of giant unilamellar vesicles

GUV were prepared using the electroformation method reported by Angelova et al. (33) using a particular protocol reported elsewhere (32). Briefly, 3 μL of a 0.2 mg/mL lipid stock solution in chloroform/methanol 2:1 was spread onto each platinum wire of an special custom built chamber (32) and the organic solvent evaporated using a stream of N_2. After this last step, the chamber was placed under vacuum for at least 2 h to ensure lack of organic solvent residues. Subsequently, the chamber was assembled and the lipid films hydrated at 70°C for 15 min using 0.2 M sucrose solution in presence of an alternate electric field (amplitude = 2 V, frequency = 10 Hz). The electric field was applied using a function generator (FG100 Vann Draper Digimess Fg 100; Stenson, Derby, UK). After this procedure the frequency of the electric field was lowered to 1 Hz for 15 min, to detach the vesicles from the Pt wires. Subsequently, the GUVs were cooled to room temperature in a time span of ~5 h in an oven (J.P. Selecta, Barcelona, Spain) using a temperature ramp (~0.2°C/min). The last step was done to achieve equilibrium conditions in our samples. Once the solution reached room temperature, the vesicles were transferred to an iso-osmolar glucose solution in a special chamber (200 μL of glucose + 50 μL of the GUVs in sucrose in each of the 8-wells of the plastic chamber used; Lab-Tek Brand Products, Naperville, IL). The density difference between the interior and exterior of the GUVs induces the vesicles to sink to the bottom of the chamber and within a few minutes the vesicles are ready to be observed using an inverted microscope.

Fluorescence microscopy experiments

An inverted confocal/two photon excitation fluorescence microscope (Zeiss-LSM 510 META NLO; Carl Zeiss, Jena, Germany) was used in our experiments. Four different set ups were used in our giant vesicle's experiments. These setups allowed us to: i), carry out combined LAURDAN and DiI_{C18} fluorescent images of the GUVs; ii), carry out two color experiments using DiI_{C18} and Alexa 488 labeled cholera toxin; iii), measure LAURDAN intensity images to compute LAURDAN generalized polarization (GP) images (see below); and iv), to measure NBD-PC labeled GUVs. The measurements described in the first case are important to obtain a spatial correlation between the particular locations of the two fluorescent probes (LAURDAN and DiI_{C18}) in the lipid membranes. In this last case, the excitation wavelengths were 543 nm (for DiI_{C18} in one photon excitation mode) and 780 nm (for LAURDAN in two photon excitation mode). The different excitation wavelengths were directed simultaneously to the sample using

a dichroic mirror (HFTS 700/543) and the fluorescence signals were collected simultaneously in two different channels using bandpass filters of 590 ± 25 nm and 424 ± 37 nm (for DiI_{C18} and LAURDAN, respectively). The Ti:Sa laser used for two photon excitation mode was a MaiTai XF-W2S (Broadband Mai Tai with 10 W Millennia pump laser, tunable excitation range 710–980 nm; Spectra Physics, Mountain View, CA). The objective used in all the experiments was a C-Apochromat 40× water immersion, NA 1.2. For the second configuration two excitation sources were used, i.e., (488 and 543 nm, respectively). Both laser lines were reflected to the sample using a dichroic mirror (HFST 488/543/633) and the fluorescence signals were collected using multitrack mode (included in the Zeiss microscope software) into two different channels using bandpass filters of 590 ± 25 nm and 515 ± 15 nm (for DiI_{C18} and Alexa 488 labeled cholera toxin, respectively). The multitrack mode is used to avoid any leakage of fluorescence emission signal of Alexa 488 into the DiI_{C18} detection channel. The configuration used for NBD-PC measurements is similar to the aforementioned one except that only the excitation at 488 nm and the 515 ± 15 nm bandpass filter (one detection channel) is used. The GUV images included in Figs. 1, 3, 6, and 10 are representative of the whole vesicle population, obtained from three different preparations for each explored lipid mixture (50–70 GUVs selected randomly are explored per sample).

LAURDAN GP images. The LAURDAN GP denotes the position of the probe's emission spectra (34). The fluorescence emission properties of LAURDAN are sensitive to the water dipolar relaxation process that occurs in the probe's local environment (the lipid bilayer in this case). The energy of the emitting singlet state decreases when the extent of dipolar relaxation process is high. Because the extent of water dipolar relaxation observed in the solid ordered phase is very low compared to what is observed in the fluid disordered phase (the extent of water dipolar relaxation process increases) a prominent red shift in the fluorescence emission of the probe is observed when a solid ordered/fluid disordered phase transition occurs (from blue to green; almost 50 nm shift) (34). The GP function was defined analogously to the fluorescence polarization function as:

$$\mathrm{GP} = \frac{I_B - I_R}{I_B + I_R}, \tag{1}$$

where I_B and I_R correspond to the intensities at the blue and red edges of the emission spectrum (440–490 nm) using a given excitation wavelength (34–36). Because this function is related to the position of the emission spectra the observed GP values can be directly related with the lateral packing existing in lipid bilayers. High LAURDAN GP values (0.5–0.6) correspond to laterally ordered phases (solid ordered-like) whereas low LAURDAN GP values (<0.2) correspond to fluid disordered-like phases (34).

LAURDAN GP images allow us to spatially correlate the GP function in a given membrane (37). The two photon excitation LAURDAN GP images were obtained using a Zeiss -LSM 510 META NLO microscope (Carl Zeiss, Germany). The LAURDAN GP images were computed using fluorescence intensity images obtained simultaneously in the blue and red regions of the probe emission spectra (bandpass filters 428 ± 37 nm and 515 ± 15 nm, respectively in our case), using 780 nm as excitation wavelength. To avoid the photoselection effect in the measured GP at the GUVs equatorial plane (34) the excitation light was circularly polarized in the *x-y* plane using a quarter wave plate. The computation of the GP images was carried out using the SimFCS package of Globals for Images software developed at the Laboratory for Fluorescence Dynamics (University of Irvine, California). The GP images were calibrated with a correcting factor G obtained by from a LAURDAN GP standard (LAURDAN solution in DMSO, GP = 0.006).

LAURDAN photoselection effect. The lack of fluorescence in the solid ordered phase domains due to the well described photoselection effect (37), is generally observed in the LAURDAN fluorescence images obtained at the polar region of the GUVs. This phenomenon is used as a qualitative criterion, to complement the information obtained from the shift in LAURDAN emission spectrum (37). Particularly, the photoselection effect is related to the probe orientation in the lipid membrane and is used in our experiments to gain further information about the lateral packing features of particular regions of the lipid membrane.

DCS experiments

Calorimetric scans were carried out on a Microcal VP-DSC (Northampton, MA). To protect the sensitive cells of the VP-DSC at temperatures <0°C one has to prevent freezing of the cell content. Therefore, the cells were filled with an ethylene glycol/H_2O 40:60 v/v mixture with a freezing point of ~−23°C. The sample solutions were filled into a closed steel capillary that was inserted into the sample cell of the VP-DSC. Freezing inside the capillary would not damage the sample cell. However, due to the small sample size one typically does not observe freezing of the sample solution. The capillary of the VP-DSC and also the sample cell of the N-DSCII were filled with a solution of multilamellar vesicles (MLVs) of the desire lipid mixture (10 mM lipid concentration). To prepare the MLVs solutions, the proper amount of lipid from the stock solution in organic solvent was evaporated in a glass tube and kept under vacuum for several hours. The lipids were then hydrated with preheated, bi-distilled water (90°C) for ~30 min and then stirred for ~30 min. After this procedure the lipid solutions were ready to use. Calorimetric scans were carried out at scan rates of 15°/h assuring thermodynamic equilibrium conditions.

FTIR experiments

The FTIR experiments were carried out using deuterated POPC (d31-POPC) instead of POPC. The carbon-deuterium stretching vibrations in the FTIR spectrum are shifted toward lower wavenumbers in respect to the carbon-hydrogen vibrations, due to the bigger mass of deuterium. This shift allows separating the melting of the deuterated chains from the melting of the undeuterated chains. In other words, the POPC melting can be monitored independently from the pb-cerebrosides melting, something that it is not possible to achieve using DSC. However, it has to be mentioned that only one chain of the POPC is deuterated. The last fact produces some signal from the POPC undeuterated lipid chains in the pb-cerebrosides fraction. However, still the chain melting events of cerebroside rich regions can be obtained accurately, even at low cerebroside molar fraction. Scans were carried out in a custom-built sample chamber with a water bath-driven temperature control device mounted in a Vertex70 FTIR spectrometer (Bruker Optics, Bremen, Germany) equipped with a mercury/cadmium/telluride detector. The sample solutions consisted of MLVs vesicles (final lipid concentration = 50 mg/mL). To produce these solutions, proper amounts of POPC and pb-cerebrosides (with or without cholesterol) where mixed from the stock solutions and evaporated under a stream of nitrogen. These dry lipid mixtures were kept under vacuum over night. The lipid samples were hydrated in bi-distilled water at temperatures above the phase transition of the high temperature melting lipid component and stirred gently for 30 min. After the last procedure five freeze-thaw cycles were applied to the lipid samples. Once the liposome solutions were ready for the experiments, 10 μL of lipid solution were added between two CaF_2 windows and the chamber was sealed properly. The spectrometer was flushed with nitrogen starting 30 min before the measurements and during the measurements, to minimize water vapor noise on the spectrum. The scans were carried out at a rate of 40°/h (30 scans were averaged for each temperature point) assuring thermodynamic equilibrium during the experiments. The temperature in the sample was determined using a reference scan, in which a thermocouple was inserted between the two CaF_2 glasses of the sample compartment. The obtained spectra were evaluated with a difference spectra method in the following way: a spectrum at temperatures below the phase coexistence regime (−7 to −6°C) was chosen as a reference and the area of the CH_2 or CD_2 stretch vibrational peaks (obtained at 2850 cm^{-1} and 2100 cm^{-1}, respectively) normalized to 1 cm^{-1}. The reference spectrum was then subtracted from the spectra obtained at the different temperatures. The total integrated area of the difference spectrum is zero with equal positive and

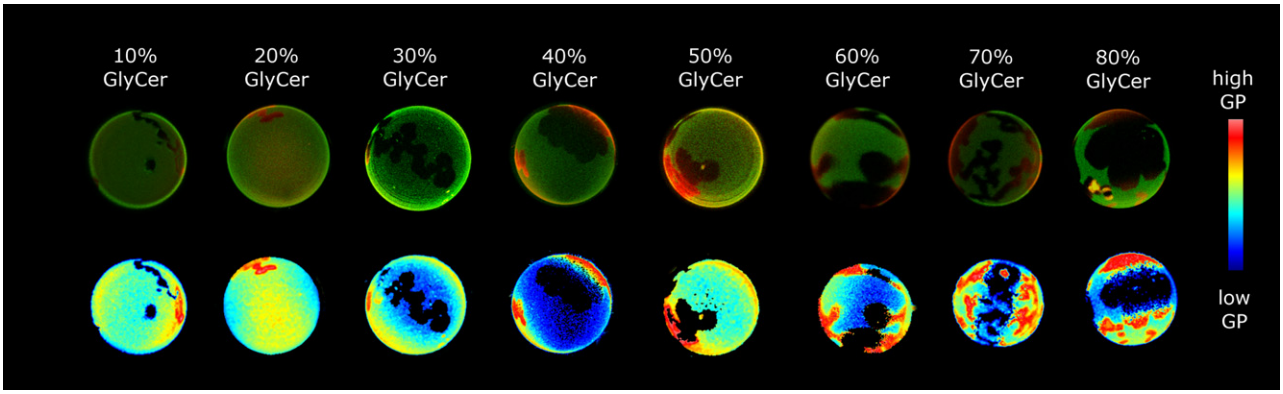

FIGURE 1 Representative two photon excitation fluorescence images showing the lateral pattern of GUVs composed of POPC with different amounts of pb-cerebrosides at 20°C. (*Top row*) LAURDAN fluorescence intensity images (false color representation) obtained with the two emission channel configuration (see Materials and Methods). Green color corresponds to liquid disordered phase domains, red color corresponds to solid ordered phase domains. Notice the strong photoselection effect in the solid ordered phase. (*Bottom row*) Computed LAURDAN GP images. The red areas correspond to high (solid ordered) GP values. Scale bar = 20 μM.

negative contributions. The corresponding positive area contributions under the peaks were used as a measure of the spectral changes (38). A plot of the change in peak area versus temperature and its derivation can then be used to interpret the lipid melting events in the membranes.

RESULTS

POPC/pb-cerebrosides mixture

Fluorescence microscopy experiments

Two photon excitation microscopy images of LAURDAN-labeled GUVs composed of different POPC/pb-cerebrosides ratios were taken at 20°C. The results are displayed in Fig. 1. The fluorescence images show phase separation phenomenon characterized by the presence of elongate shaped domains, occurring in a composition range from 0.1 to 0.9 molar fractions of cerebroside. The area fraction of these domains increases by increasing the pb-cerebroside molar fraction. Below a pb-cerebroside molar fraction of 0.1 the distribution of the probes in the GUVs is homogeneous. The observed domains span the lipid bilayer in all cases as was reported previously for other lipid mixtures (39,40).

To characterize the nature of the lipid phase coexistence scenario observed in GUVs, LAURDAN GP images were acquired from the GUV fluorescence images. The different membrane regions observed in the GUVs (Fig. 1) show high and low GP values (~0.6 and ~−0.3, respectively; Fig. 2). This is in agreement with GP values observed previously in lipid mixtures that display fluid disordered/solid ordered phase coexistence (39–41). Taking into account the last observation and the high difference in the main phase transition temperature for these two pure lipids (porcine cerebroside and POPC; 64°C vs. −2.6°C, respectively) we conclude that: i), the high GP areas correspond to pb-cerebrosides enriched solid ordered domains; and ii), the low GP areas correspond to POPC enriched liquid disordered lipid domains. This last conclusion is also supported by the fact that these two regions display a different extent of photoselection effect. The photoselection effect is particularly strong in the high GP (solid ordered) regions (Fig. 1) in agreement with previous results showing solid ordered/liquid disordered phase coexistence scenarios (37). Additionally, the GP values observed in cerebroside rich solid ordered phase at 20°C show that the extent of water dipolar relaxation process is very low (GP values between 0.5–0.6) and independent of the molar fraction of the mixture components (Fig. 2). On the other hand, the low GP values observed in the POPC rich fluid domains (~−0.3) increases at a pb-cerebrosides molar fraction >0.7 (from −0.3 to 0.17; Fig. 2).

Additionally, it was not possible to generate GUVs composed of pure pb-cerebrosides. The last finding may be due to the fact that high temperatures >70°C are required during GUV preparation to have pb-cerebrosides membranes in the liquid disordered phase (this is an important requirement for GUV preparation). These conditions are not easy

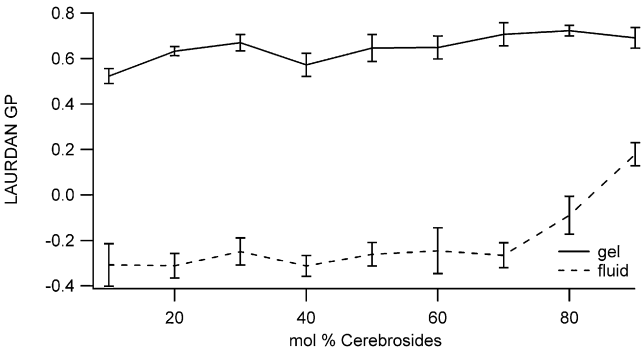

FIGURE 2 LAURDAN GP mean values of solid ordered and fluid disordered domains at different pb-cerebroside mol % in POPC/pb-pb-cerebrosides mixtures. The LAURDAN GP values are averages obtained from the individual domains (5 measurements per GUV) in 10–15 different GUVs.

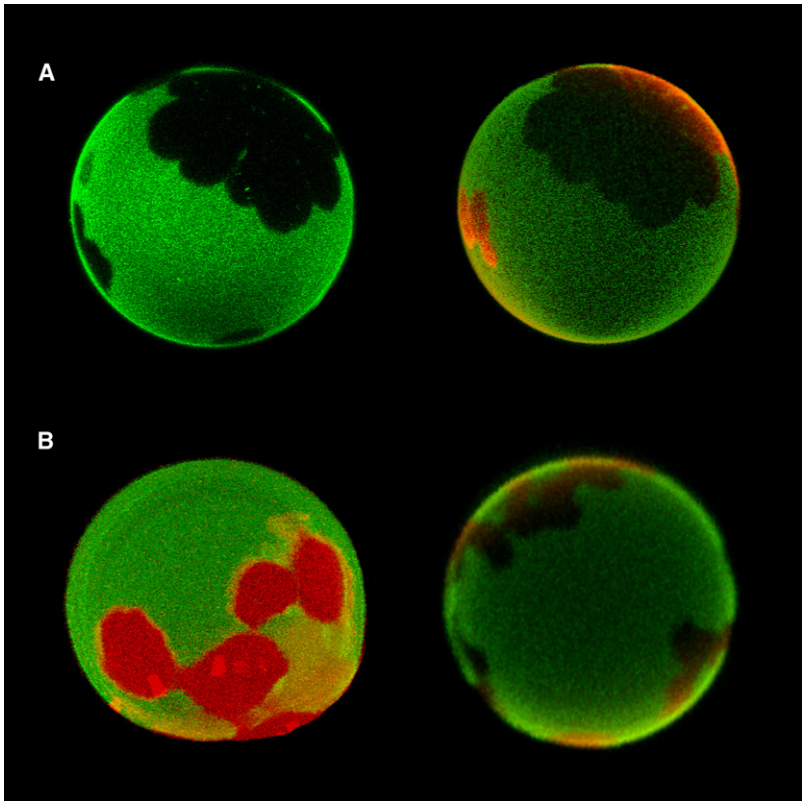

FIGURE 3 (*A*) Comparison of DiI_{C18} and LAURDAN fluorescence intensity from the same vesicle composed of POPC/pb-cerebrosides 3:2 mol. Left image showing DiI_{C18} fluorescence (*green*), right image showing LAURDAN distinct fluorescence in the fluid disordered and solid ordered domains (*green* and *red* respectively). (*B*) Comparison of DiI_{C18}/Alexa 488 cholera toxin and LAURDAN fluorescence intensity in vesicles composed of POPC/pb-cerebrosides 3:2 mol, Left image showing DiI_{C18} fluorescence (*green*) and Alexa 488 cholera toxin (*red*), right image showing LAURDAN distinct fluorescence in the fluid disordered and solid ordered domains (*green* and *red*, respectively). Scale bar = 20 μM.

to achieve in our electroformation chamber due to the massive water evaporation of water during preparation (and are particularly critical at high cerebroside molar fractions, i.e., 0.8–0.9; see Discussion). An additional explanation is that this compositionally complex pb-cerebrosides mixture alone may also form nonbilayer structures that can destabilize the GUV during preparation (26,28).

Experiments using $DiI\text{-}_{C18}$ labeled GUVs are shown in Fig. 3. In this case, the fluorescent probe shows a preferential partition into one of the lipid phases. By comparing the DiI_{C18}-labeled GUVs images with those obtained using LAURDAN it becomes clear that DiI_{C18} probe preferentially partitions into the liquid disordered phase (Fig. 3 *A*). Moreover, experiments using GUVS labeled with the NBD-PC fluorescent probe show a preferential partition of this probe to liquid disordered phases in agreement with that reported previously for similar mixtures (see Fig. 10 *A*) (31). Additional experiments were done by incorporation of 1 mol % of G_{M1} in the POPC/cerebroside mixture using fluorescent labeled cholera toxin as a marker (Fig. 3 *B*). G_{M1} also belongs to the sphingolipid family (i.e., it is a ganglioside) and it is very likely that the sphingolipid moiety will partition to cerebroside rich areas in our model membrane system. Indeed, our experimental results show that the fluorescent labeled cholera toxin binds to the solid ordered like (cerebroside enriched) areas. This finding indicates that the G_{M1}/cholera toxin labeling approach can be used as a marker for cerebroside enriched solid ordered phases in the POPC/cerebroside mixture (notice that no fluorescence signal from the fluorescently labeled cholera toxin is observed in the liquid disordered regions), whereas DiI_{C18} can be used to label POPC-enriched liquid disordered phase areas. This result shows an alternative labeling option using epifluorescence or confocal microscopy experiments when two-photon excitation microscopy is not available.

DSC experiments

DSC scans on MLVs composed of POPC/pb-cerebrosides mixtures at different lipid component mixing ratio are shown in Fig. 4. The samples composed of pure POPC show a transition maximum at −2.6°C, whereas those composed of pb-cerebrosides only display a main phase transition at 64°C. The DSC scan of MLVs containing only pb-cerebrosides displays two peaks (Fig. 4). The last may reflect the particular compositional complexity of the cerebroside mixture (see Materials and Methods). When the POPC/cerebroside mixtures are explored, two different peaks can be distinguished in the thermograms. The position and width of these two peaks show a clear dependence on the molar fraction of the components. For instance, at a molar fraction of pb-cerebrosides ranging from 0 to 0.5, the low temperature peak shows no shift in temperature, which is a typical scenario for a low miscibility of the two lipid components in the solid ordered phase. The upper temperature limit of the heat capacity profiles increases with increasing pb-cerebroside content, indicating a much better miscibility in the

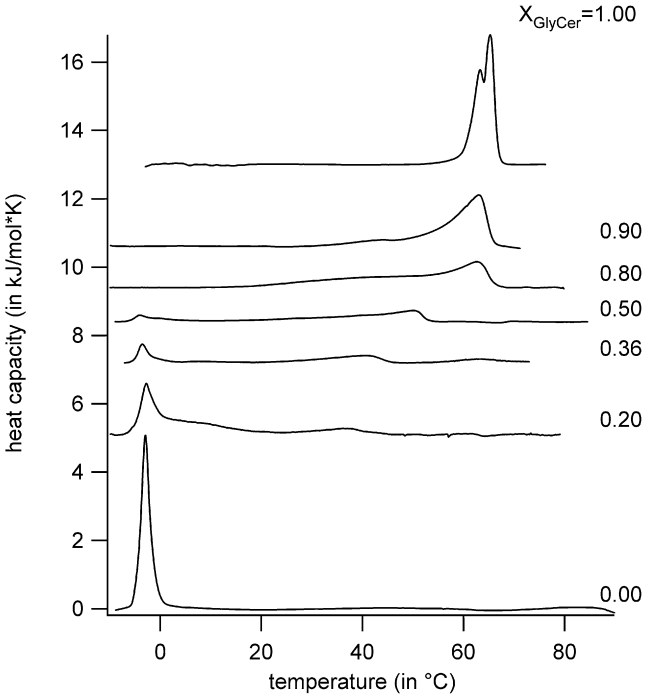

FIGURE 4 DSC thermograms of multilamellar vesicles composed of POPC/pb-cerebroside mixtures at different pb-cerebroside molar ratios.

liquid disordered phase. From our data it is clear that the fraction of POPC lipids in the fluid state is always higher than the fraction of cerebroside lipids. This means that the fraction of POPC in the liquid disordered domains is always higher than in the solid ordered domains. For pb-cerebrosides one sees the opposite. Solid ordered domains are always richer in pb-cerebrosides than liquid disordered domains. This is also confirmed by the FTIR measurements (see below). These results are similar to those reported using the same experimental technique from Curatolo (7) where cerebroside from bovine sources were mixed with POPC. Our DSC results are in agreement with those obtained in GUVs, except at high molar fractions of cerebrosides (i.e., 0.8 and 0.9). For these molar fractions, the DSC experiments suggest at 20°C existence of a solid ordered phase. However, the observed GUVs population consistently shows coexistence of two regions with different lipid packing.

FTIR experiments

FTIR experiments were carried out to explore the temperature behavior of POPC/pb-cerebrosides mixtures. As a representative data the melting curve of d31-POPC/cerebroside 4:1 mol is shown in Fig. 5. The deuterated POPC profile shows a strong increase of the wavenumber at ~−5°C, corresponding to the larger fraction of POPC in the regions that melt at low temperatures (Fig. 5, *left panel*). The melting of the pb-cerebrosides takes place over a larger temperature interval (Fig. 5, *right panel*). The derivative curves indicate the change of the fraction of fluid lipid of the components. These curves can be considered as melting profiles of the individual components (Fig. 6, *lower panels*). It can be seen that the pb-cerebrosides mostly melt at higher temperature. The investigation of the derivative of the wavenumber change for the undeuterated component of the mixture shows a broad peak with a maximum at 30°C. This temperature is in agreement with the upper peak observed in the DSC experiments at the same molar fraction (Fig. 4). Additionally the contribution of the nondeuterated chain of POPC can be followed showing a prominent peak at −3°C, where the transition of this lipid occurs (Fig. 5).

POPC/pb-cerebrosides/cholesterol mixture

Fluorescence microscopy experiments

Fig. 6 shows two photon excitation fluorescence intensity and GP images of LAURDAN-labeled GUVs composed of POPC/pb-cerebrosides 4:1 containing different proportions of cholesterol. These images were obtained at 20°C. From these experiments it is obvious that a phase separation pattern is observable up to 30 mol % of cholesterol in the membrane. The lipid domains below 30 mol % have an elongated shape

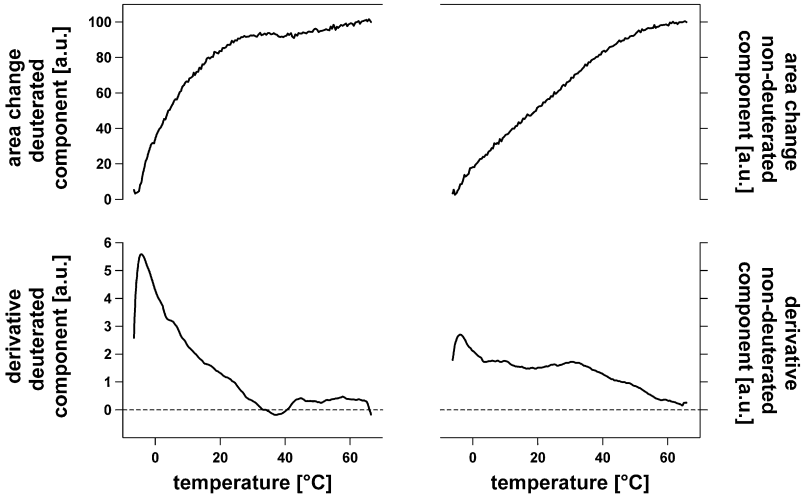

FIGURE 5 Thermal behavior of MLVs composed of dPOPC-d31/pb-cerebrosides 4:1 mol. The values were obtained from area changes of the FTIR spectrum peak at 2920 cm^{-1} (undeuterated lipid chains) and at 2195 cm^{-1} (deuterated lipid chains). The figure also shows their corresponding derivatives.

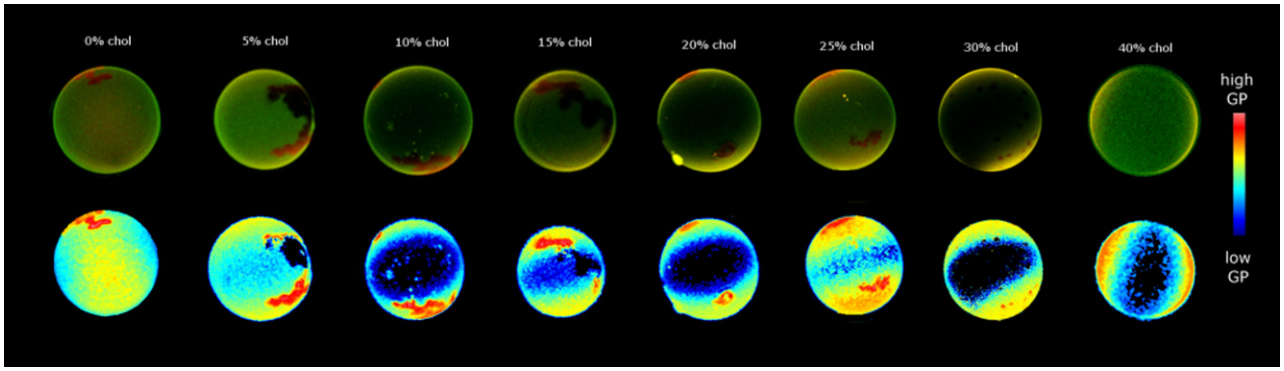

FIGURE 6 Two photon microscopy pictures of POPC/pb-cerebrosides (4:1 mol ratio) GUVs containing different amounts of cholesterol. *Top row*: LAURDAN fluorescence intensity images (false color representation) obtained with the two emission channel configuration (see Materials and Methods). Green and red color corresponds to disordered and ordered lipid phases. *Bottom row*: Computed LAURDAN GP images. Scale bar = 20 μM.

resembling the shapes observed in the POPC/cerebroside binary mixture. However, at 30 mol % formation of round domains becomes the dominant scenario (although still some vesicles displaying elongated lipid domains for the same mixture molar ratio). The domains observed in the GUVs span the lipid bilayer (are symmetric) in agreement with previous data (31). With further addition of cholesterol (up to 40 mol %) the presence of micrometer size domains vanishes, rendering a homogeneous distribution of the probe in the membrane (as can be seen in the microscope, where the resolution limit is ~300 nm in the radial direction). Fig. 7 shows the evolution of the GP values in the two observed membrane regions as cholesterol molar fraction is increased in the lipid mixture. The LAURDAN GP values for the cerebroside enriched phase display a constant high GP value of ~0.6 up to a 25 mol % of cholesterol, showing a very low amount of water dipolar relaxation process in the membrane region where the probe is located (just below the polar headgroup of the lipids (34)). This corresponds very well with the presence of a single solid ordered phase. The GP value of these rigid domains drops at 30 mol % of cholesterol, reaching an even lower value when cholesterol is rising to 40 mol %. In this cholesterol regime (30–40 mol %) the decrease of the GP values up to 0.2 shows a gradual increase of the extent of water dipolar relaxation processes in the cerebroside enriched domains. This observation suggests that a gradual change from a solid ordered phase to a liquid ordered-like phase may occur in these lipid membrane regions as cholesterol concentration augments from 25 to 40 mol % of cholesterol. On the other hand, the LAURDAN GP values for the liquid disordered phase increase in a quasi linear manner (particularly above 5 mol % of cholesterol) from −0.3 to ~0.2. The last indicates a strong decrease in the extent of the water relaxation processes present in the membrane as the cholesterol percentage increase in the mixture. The last scenario can be interpreted as a gradual formation of a liquid ordered phase from the POPC enriched liquid disordered phase.

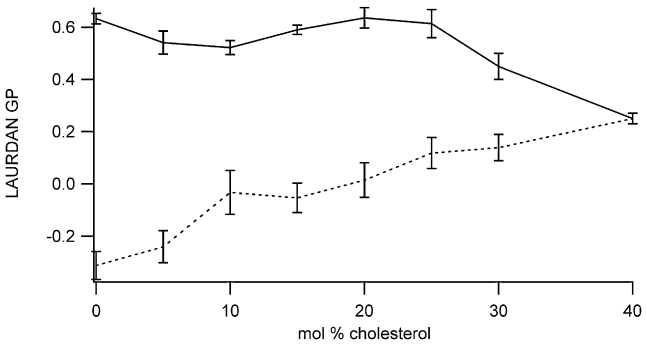

FIGURE 7 LAURDAN GP means values of the coexisting domains in POPC/pb-cerebrosides 4:1 mol mixture containing different amounts of cholesterol. The GP values are averages obtained from 10 to 15 GUVs per lipid mixing ratio.

An interesting feature of this mixture is that observed between 30 and 40 mol % of cholesterol. In this case two different micrometer-sized regions with distinguishable GP values (~0.15 and 0.4) coexist in the membrane. Based on the obtained GP values, we conclude that these two areas represent liquid ordered-like phases with different extent of water dipolar relaxation process. Interestingly, at 40 mol % the presence of these micrometer-sized domains is abolished in the membrane (the probe distribution in the membrane is even) and a single LAURDAN GP value of ~0.2 is measured. The last scenario correlates with presence of a single liquid ordered-like phase (considering our resolution limit, i.e., 300 nm radial in our microscope).

DCS experiments

The impact of cholesterol on a POPC/pb-cerebrosides 4:1 mol mixture has also been investigated by DSC and the results are shown in Fig. 8. When the amount of cholesterol is increased different effects on both peaks were observed in the lipid mixture. The cholesterol effect on the low temperature peak is the more dramatic showing a broadening in the peak width and a shift to higher temperatures. The broadening of the low temperature peak and the temperature shift (~8°C) are signatures of the presence of cholesterol and further generation of

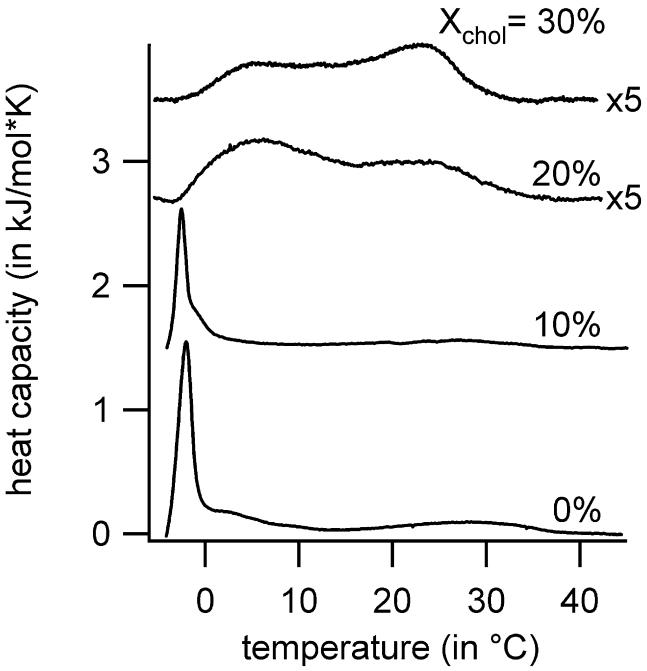

FIGURE 8 DSC thermograms of multilamellar vesicles composed of POPC/pb-cerebroside 4:1 mol mixture containing different cholesterol concentrations. The two uppermost traces were multiplied by a factor of five for enhancement and clarity.

a liquid ordered phase particularly at and above 20 mol % (Fig. 8). This data is in agreement with the LAURDAN GP measurements carried out on GUVs (Fig. 7). On the other hand, addition of cholesterol up to 30 mol % slightly shifts the melting peak (~2.5°C) that correspond to the transition of a cerebroside enriched phase to lower temperatures, with no evident changes in the broadening of the transition peaks. Above 30 mol % cholesterol it is very difficult to trace the endotherm because the thermogram is almost overlapping the baseline (not shown). The behavior of the peak located

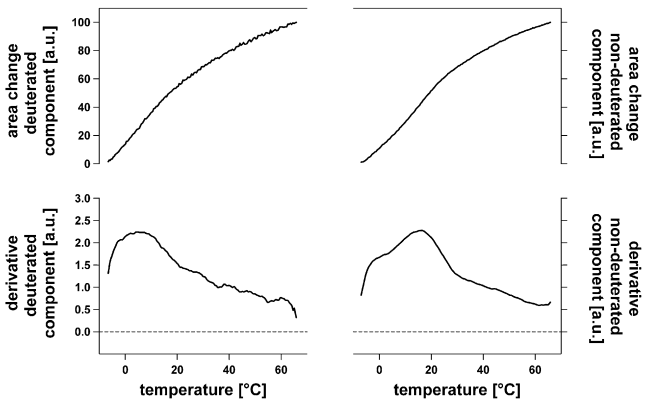

FIGURE 9 Thermal behavior of MLVs composed of dPOPC-d31/pb-cerebrosides 4:1 containing 26% cholesterol. The values were obtained from area changes of the FTIR spectrum peak at 2920 cm^{-1} (undeuterated lipid chains) and at 2195 cm^{-1} (deuterated lipid chains). The figure also shows their corresponding derivatives.

at higher temperatures suggests a strong destabilization of the solid ordered-like cerebroside enriched regions at high cholesterol concentrations (above 30 mol %). This can be interpreted as the formation of a single liquid ordered phase in agreement with the LAURDAN GP experiments.

FTIR experiments

Results of the FTIR temperature scans on POPC/pb-cerebrosides 8:2 mol lipid mixture containing 26% cholesterol are shown in Fig. 9. The derivation of the change in wavenumber for the deuterated component shows a broad peak with a maximum at 4°C in agreement with that observed for POPC enriched regions in the DSC experiments. On the other hand, the derivation of the FTIR data for the undeuterated component shows a rather broad distribution with a peak observed at ~20°C. The FTIR data shows that cholesterol affects both peaks in the lipid mixture melting profile. This is in agreement with the observations obtained both with DSC and fluorescence microscopy experiments.

DISCUSSION

POPC/pb-cerebrosides mixture

Based on the experimental results reported in this study (visual information obtained on the level of single vesicles and bulk-mean parameters obtained from solutions of liposomes) we can conclude that the POPC/pb-cerebroside mixture displays solid ordered/liquid disordered phase separation over a broad range of temperatures and compositions. This observation is similar to that reported Curatolo (7), where cerebrosides from bovine source were mixed with POPC. Our results add information about domain morphological features for this lipid mixture at different molar fraction unavailable previously; information that it is relevant for comparison with previous results obtained from our laboratory for ceramide-containing similar mixtures (32) using a related experimental approach (see below).

In the following, we discuss some details about the lateral structural features of the different temperature and composition regimes observed for the POPC/pb-cerebroside mixture. This discussion also emphasizes some practical findings obtained by comparing results obtained among the different experimental techniques.

The low temperature regime

The POPC/cerebroside mixture shows solid ordered phase immiscibility up to high proportions of cerebroside at low temperatures, as observed in the experiments using DSC and FTIR techniques (Figs. 4 and 6). The last conclusion suggests that the POPC solid ordered phase does not contain significant amounts of pb-cerebrosides and nearly melts as pure POPC. This last phenomenon was also reported in other lipid mixtures that display high differences between the individual lipid melting points (42,43). Unfortunately, and for

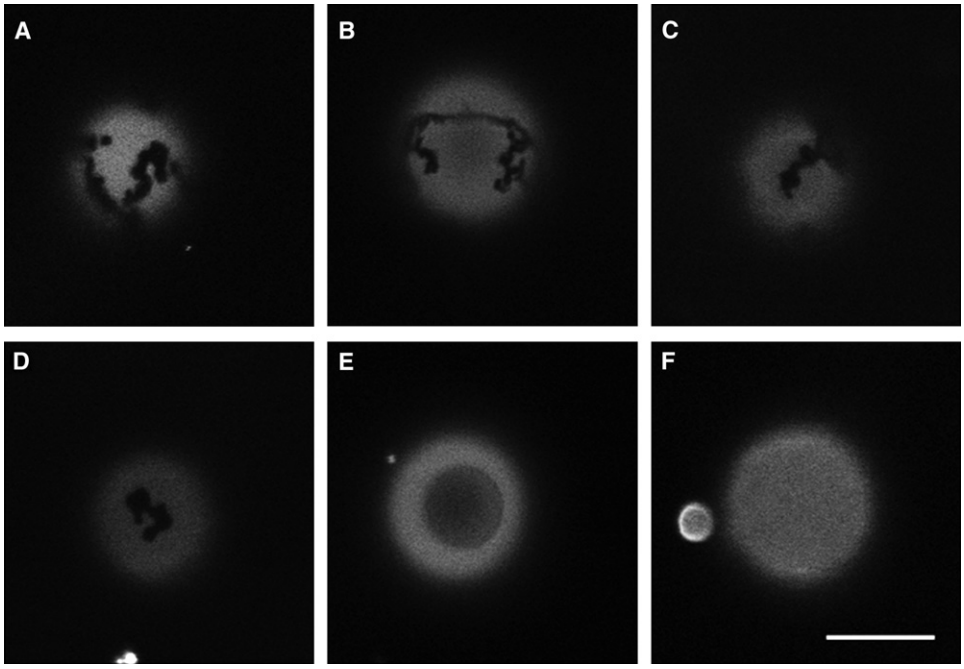

FIGURE 10 NBD-PC fluorescence intensity images of GUVs composed POPC/pb-cerebrosides 4:1 mol containing (*A*) 0 mol %, (*B*) 15 mol %, (*C*) 20 mol %, (*D*) 25 mol %, (*E*) 30 mol %, and (*F*) 40 mol % cholesterol. Scale bar = 20 μM.

technical reasons, it was not possible to visually explore this low temperature regime using GUVs/fluorescence microscopy (this regime exists below 0°C and GUVs experiments below this temperatures are not possible to carry out) as was done previously for DPPC/DPPE and DSPC/DMPC mixtures (39,40).

Room temperature regime

As we mentioned above, independent of the difference source of cerebrosides (porcine in our case), the phase coexistence regime observed in our experiments is in line with that reported by Curatolo (7) for POPC/bovine brain cerebroside mixtures. For this mixture, Curatolo proposed nonideal behavior in the liquid disordered phase that might lead to cerebroside clustering (7). With the aim to explore if this phenomenon can be observed in our POPC/pb-cerebroside mixture at room temperature (below a pb-cerebroside molar fraction of 0.1), we exploited the particular spatial/temporal resolution of our fluorescence microscope. Fluorescence microscopy has an intrinsic resolution limit above 300 nm (in the image plane) with a temporal resolution of the order of 10 s (that is the rate of image acquisition in our particular case). By exploring the images obtained in this particular regime we observed a homogeneous fluorescent distribution (also GP) in the GUVs (data not shown). The last suggest that the proposed cerebroside clustering (7) is transient and non detectable by the microscopy technique used here. In this respect, it is interesting to point out that this phenomenon was not observed in planar membranes composed of other cerebroside containing binary lipid mixtures using AFM (30). The last technique has a higher (subnanometer) resolution but a low temporal resolution (min) compared to fluorescence microscopy. Based on these observations we considered that measurements of probe diffusion coefficient using fluorescence correlation spectroscopy may be the best way to explore this phenomenon using microscopy based techniques. Preliminary experiments in this direction are currently taking place in our laboratory.

In general, the correlation among the results obtained from the different techniques used in this study is very good. However, we notice some discrepancies between the results obtained from GUVs experiments and DSC at high pb-cerebroside molar fractions (0.8 and 0.9). For example, it is somewhat surprising to still observe liquid disordered-like domains at 20°C in representative GUV populations at these high pb-cerebroside molar fractions (Fig. 1) because the information obtained by DSC and FTIR suggest the presence of a single solid ordered phase at this temperature and lipid compositions. We speculate that this observation can be related to the difficulties in preparing GUVs at the higher molar fractions of pb-cerebroside, already mentioned in the result section (e.g., pure cerebroside mixtures do not form GUVs). In our custom built electroformation chamber the higher temperature we can reach, without massive water evaporation during GUV preparation, is 70°C. This temperature overlaps the end of the transition temperature regime observed by DSC for these high molar fractions-cerebroside containing mixtures. It is well known that to prepare GUVs (or other liposome preparations) the temperature must be well above the (higher) main phase transition of the lipid mixture of interest. In our experiments for the higher cerebroside molar fractions (0.8 and 0.9), this condition is not well satisfied, and presence of metastable phases in the membrane can not be completely discarded. The thermotropic properties of many cerebrosides have previously been shown to be polymorphic and largely dependent on

the sample history (44,45). It is important to remark that the experimental situation for preparation of compositionally related MLVs (used by the DSC and FTIR experiments) is very different to that used in GUVs because the temperature used for preparation (90°C) is indeed well above the higher transition temperatures observed by DSC. Additionally, mechanical forces (stirring) were applied during the hydration of the MLV samples. These conditions assure proper lipid equilibration in the MLVs final preparation. Finally, it is also important to mention that we are confident that the temperature used for electroformation of GUVs containing lower molar fractions of cerebroside (below 0.8–0.9) preclude formation of metastable phases in the GUVs. The last fact is strongly supported by the good agreement among the results obtained by the different experimental techniques used in this study.

The detailed visual information obtained from the GUV experiments help to establish a comparison with previous data obtained in similar systems. In our particular case we notice that the observed solid ordered domains span the lipid bilayer, independent of the cerebroside molar fractions in the mixture as was reported for GUVs containing other lipid mixtures (39,40). This information is in line with the results presented by Lin et al. (31), where presence of symmetric domains were observed for GUVs composed of POPC/bovine cerebrosides 65:35 mol %. These authors report that the solid ordered domains in GUVs were symmetric and different to the domain asymmetric nature they observed in planar supported membranes for the same mixture (31). Because our results show consistently solid ordered domain symmetry in GUVs composed of different POPC/cerebroside mixtures, we can discard any dependence of this phenomenon with the amount of cerebroside present in the membrane. The last suggest that the solid ordered domain asymmetric nature observed in the supported membranes may be associated to the particular characteristic of the model membrane and/or the preparation procedure.

Comparison with porcine brain ceramide/POPC mixtures

By comparing the POPC/pb-cerebroside data with that reported from our laboratory for POPC/Porcine brain ceramide mixtures (32), it is very obvious the impact that the galactosyl moiety exerts (our pb-cerebroside mixture is galactosyl-ceramide) on the physical properties of the sphingolipid-containing membranes. For example, in mixtures of POPC/porcine brain ceramide it is not possible to incorporate more than 25 mol % of porcine brain ceramide in the membrane (32), whereas pb-cerebroside can incorporate up to 90 mol % with POPC. These observations are well in line with the changes imposed in the lipid molecular structure (reflected in the critical packing parameter of the different lipids) by incorporating a galactosyl group in the ceramide moiety. On the other hand, it is important to notice some similarities in the sphingolipid-rich solid ordered phase domain shapes between these two different mixtures. The last may indicate maintenance of some of the supramolecular features of the sphingolipid rich solid ordered domains, perhaps those related to the formation of intermolecular hydrogen bonds (46), even though the nature of the sphingolipid polar headgroup changes.

POPC/pb-cerebrosides/cholesterol mixtures

At a first glance, the effect of cholesterol on the lateral structure of the cerebroside containing mixtures can be placed in between those observed from porcine brain ceramide and sphingomyelin containing mixtures. For example, the particular lipid domain shape patterns observed in the formation of the liquid ordered/liquid disordered phase coexistence in mixtures of phospholipids, sphingomyelin and cholesterol (47,48) are not observed in the pb-cerebroside containing mixtures up to high concentrations of cholesterol. Additionally, some of the features (domain shape, nature of the phase coexistence regions) observed for POPC/porcine brain ceramide/cholesterol mixture can be found in the corresponding pb-cerebroside containing mixture, even though substantial differences can also be observed between these two mixtures. For example, POPC/porcine brain ceramides GUVs display solid ordered and liquid ordered phase coexistence when 10–20 mol % cholesterol are present in the membranes (32), similar to that observed for POPC/pb-cerebrosides containing similar cholesterol molar fractions. On the other hand, the particular three membrane region pattern with high GP values, reported for the POPC/porcine brain ceramide mixture containing >20 mol % cholesterol (32), was absent in the pb-cerebroside containing lipid mixture at similar cholesterol content. Instead, the POPC/pb-cerebroside mixtures show coexistence of two different micrometer sized liquid ordered-like phases when the cholesterol concentration is between 30–40 mol % (Figs. 6 and 7). This last situation is not unexpected for a multicomponent lipid mixture (pb-cerebroside is a mixture of lipids, see material section), but was not reported before for cerebroside containing lipid mixtures. Importantly, this particular phase scenario remains up to 40 mol % cholesterol, where a single liquid ordered phase is detected (Figs. 6 and 7). We interpret this phenomenon as liquid-liquid immiscibility with a mixing gap that closes on temperature increases. The last explain our experimental observations for the 30–40 mol % cholesterol concentration range, i.e., why, on a further increase of cholesterol concentration, the membrane scenario change from a regime characterized by the coexistence of two distinct liquid ordered-like phases to a regime characterized by the presence of a single liquid ordered-like phase. Liquid-liquid immiscibility (or heterogeneity) has been described previously in membranes, e.g., ternary mixtures of sphingomyelin, POPC, and cholesterol (49), in 1,2-di-(13Z-docosenoyl)-sn-glycero-3-phosphocholine (DEPC)-1,2-dipalmitoyl-sn-glycero-3-phosphoethanolamine (DPPE) mixtures

(50), and in monolayers made of dihydrocholesterol and DMPC (51). Lee (50) showed how the miscibility gap in the DEPC-DPPE system closes with increasing temperature until it reaches a critical point. This last system most likely describes an immiscibility of two liquid disordered phases, whereas the other two systems more likely display liquid ordered-liquid disordered immiscibility. Close to the critical point the distinction between these different kinds of two-phase regions (liquid disordered-liquid disordered and liquid disordered-liquid ordered) continuously vanishes.

The difference in the lateral patterns observed for POPC/porcine brain ceramides/cholesterol and POPC/pb-cerebrosides/cholesterol GUVs may originate from their different headgroup moiety, as the hydrophobic part of these lipid molecules is the same. Several publications report that ceramides displace cholesterol from ordered bilayers (52,53). Ali et al (52) stated that ceramides have a higher affinity to ordered bilayers than cholesterol and that both molecules have very small polar headgroups compared to their nonpolar moieties. To prevent the exposure of the hydrophobic bodies to the surrounding water, ceramides, and cholesterol tend to shield their small headgroups below the headgroups of the neighboring lipids, a phenomenon that may be explained by the umbrella model (54). However, this effect is expected to be weak in the case of cerebrosides because the characteristics of the polar headgroup. On the other hand, these sphingolipids (cerebrosides and ceramides) have the capability to establish intermolecular hydrogen bonding (46), a phenomenon that locally strengthens the supramolecular interactions in a sphingolipid rich lipid domain. Combination of these two effects in different extents might explain the formation and persistence of the solid ordered/liquid ordered phase coexistence scenario observed for POPC/porcine brain ceramide/chol (up to 20 mol % cholesterol) (32) and POPC/pb-cerebroside mixture (up to 25 mol % of cholesterol). This situation seems to differ to that reported for sphingomyelin (that contains phosphatidylcholine in the polar headgroup) containing related mixtures, where coexistence of liquid ordered/liquid disordered phases (absent in our mixtures) is observed at low concentrations of cholesterol (55).

The additional observation of two different liquid ordered-like phases between 30–40 mol % of cholesterol in POPC/pb-cerebrosides mixtures is remarkable, and can be expected to occur in a multicomponent mixture containing cholesterol. The formation of this phase coexistence scenario from a solid ordered/liquid ordered pattern can be interpreted as the gradual weakening of the intermolecular interactions among pb-cerebrosides molecules in the solid ordered phase caused by cholesterol. For this effect to take place, a relative high concentration of cholesterol in the mixture is necessary (~30 mol %). Further increase in the cholesterol concentration (~40 mol %) generate a homogeneous probe distribution suggesting the presence of a single liquid ordered phase.

The impact of PC phospholipid alkyl chain saturation on the lateral domain pattern of lipids in mixtures containing phospholipids, cerebroside, and cholesterol has been investigated recently by Lin et al. (31). These authors reported for the POPC/cerebroside/cholesterol mixture a transition from L-L to L, occurring at 17.5 mol % of cholesterol when the cerebroside/POPC ratio reaches ~4:1 mol (notice that the authors did not discussed the detailed nature of the coexisting phases for the mixtures containing cholesterol, i.e., ordered or disordered) (31). This last observation disagrees with the results obtained in our experiments for equivalent lipid mixtures, where a similar phase transition (two distinct liquid phases to one) is observed at 40 mol % of cholesterol. Because the conclusions of Lin et al. (31) relay the determination of such phase transition on the partition of NBD-PC probe (AFM experiments can not be carried out because the membrane became too soft), we decided to carry out the same type of experiments (using NBD-PC probe) in GUVs composed of POPC/pb-cerebrosides with and without cholesterol. Fig. 10 summarizes our observations. From this control experiment it is evident that the NBD-PC fluorescent probe resembles consistently the results obtained with LAURDAN (compare Figs. 6 and 10). The last observation suggests that a difference in the composition of the cerebroside lipids (POPC and cholesterol are from the same vendor in our study and the study by Lin et al. (31)), rather than changes in the partition properties of the NBD fluorescent probe when the lipid composition change, may be the source of the differences observed in our results and the results of Lin et al. (31). The cerebroside lipids used by Lin et al. (31) are obtained from bovine source and are provided from a different vendor compared to our study. The GalCer lipids (from Matreya, Pleasant Gap, PA) used in the Lin et al. (31) study is a mixture of nonhydroxylated and hydroxylated GalCer (75% saturated and 25% singly unsaturated) with tail lengths varying from 18 to 27 carbons. On the other hand, the pb-cerebroside used in our study (from Avanti Polar Lipids) is a complex mixture of galactosyl cerebrosides with different saturated (49%; 24:0 and 22:0 the most abundant saturated chain species) and unsaturated (11%; mainly 24:1) chain lengths. However, precise information about the chain length/degree of unsaturation for the rest of the cerebroside components (40%) used in this study is not reported by the vendor company (Avanti Polar Lipids). This last fact precludes an absolute comparison between the compositions of these two sources of cerebrosides. Nevertheless it is evident from the aforementioned information that the composition of these two cerebroside lipid mixtures differs, explaining the differences observed by Lin et al. (31) and our results.

CONCLUSIONS

Of particularly relevance is the capability of the presented array of experimental techniques to ascertain the lateral scenario of compositionally complex membranes. For example, we showed that pb-cerebrosides/POPC mixtures show a solid ordered/liquid disordered phase coexistence

region in a broad range of temperature and composition in agreement with that observed in similar mixtures containing bovine brain cerebrosides (7). Incorporation of cholesterol in the POPC/pb-cerebroside mixture modifies the membrane lateral structure promoting a rich and diverse phase coexisting scenario as cholesterol concentration increases, being a relevant feature the coexistence of two distinct liquid ordered phases. Last but not least, comparison with similar ceramide-containing lipid mixtures shows the strong impact of the sphingolipid polar moiety on the lateral organization of these membranes. This may be important in relevant biological membranes (e.g., myelin in this particular case) where specific enzymes can originate spatially confined compositional fluctuations among different sphingolipid species causing local variations on the membrane lateral structure.

This work was supported by funds from BioNET (supported by the Villum Kann Rasmussen Foundation, Denmark), Forskningsrådet for Natur og Univers (FNU, Denmark), and the Danish National Research Foundation (that supports MEMPHYS-Center for Biomembrane Physics).

REFERENCES

1. Chen, Y. Q., M. A. Rafi, G. de Gala, and D. A. Wenger. 1993. Cloning and expression of cDNA encoding human galactocerebrosidase, the enzyme deficient in globoid cell leukodystrophy. *Hum. Mol. Genet.* 2:1841–1845.
2. Hansson, G. C. 1983. The subcellular localization of the glycosphingolipids in the epithelial cells of rat small intestine. *Biochim. Biophys. Acta.* 733:295–299.
3. Hauser, H., K. Howell, R. M. Dawson, and D. E. Bowyer. 1980. Rabbit small intestinal brush border membrane preparation and lipid composition. *Biochim. Biophys. Acta.* 602:567–577.
4. Norton, W. T., T. Abe, S. E. Poduslo, and G. H. DeVries. 1975. The lipid composition of isolated brain cells and axons. *J. Neurosci. Res.* 1:57–75.
5. Tan, R. X., and J. H. Chen. 2003. The cerebrosides. *Nat. Prod. Rep.* 20:509–534.
6. Johnson, A. C., A. R. McNabb, and R. J. Rossiter. 1948. Lipids of normal brain. *Biochem. J.* 43:573–577.
7. Curatolo, W. 1986. The interactions of 1-palmitoyl-2-oleylphosphatidylcholine and bovine brain cerebroside. *Biochim. Biophys. Acta.* 861:373–376.
8. Bosio, A., E. Binczek, and W. Stoffel. 1996. Functional breakdown of the lipid bilayer of the myelin membrane in central and peripheral nervous system by disrupted galactocerebroside synthesis. *Proc. Natl. Acad. Sci. USA.* 93:13280–13285.
9. Coetzee, T., N. Fujita, J. Dupree, R. Shi, A. Blight, et al. 1996. Myelination in the absence of galactocerebroside and sulfatide: normal structure with abnormal function and regional instability. *Cell.* 86:209–219.
10. Bosio, A., E. Binczek, W. F. Haupt, and W. Stoffel. 1998. Composition and biophysical properties of myelin lipid define the neurological defects in galactocerebroside- and sulfatide-deficient mice. *J. Neurochem.* 70:308–315.
11. Eto, Y., K. Suzuki, and K. Suzuki. 1970. Globoid cell leukodystrophy (Krabbe's disease): isolation of myelin with normal glycolipid composition. *J. Lipid Res.* 11:473–479.
12. Suzuki, K. 1998. Twenty five years of the "psychosine hypothesis": a personal perspective of its history and present status. *Neurochem. Res.* 23:251–259.
13. Suzuki, K., and Y. Suzuki. 1970. Globoid cell leukodystrophy (Krabbe's disease): deficiency of galactocerebroside beta-galactosidase. *Proc. Natl. Acad. Sci. USA.* 66:302–309.
14. Suzuki, K., and M. T. Vanier. 1998. Induced mouse models of abnormal sphingolipid metabolism. *J. Biochem. (Tokyo).* 124:8–19.
15. Beier, U. H., and T. Gorogh. 2005. Implications of galactocerebrosidase and galactosylcerebroside metabolism in cancer cells. *Int. J. Cancer.* 115:6–10.
16. Bhat, S., S. L. Spitalnik, F. Gonzalez-Scarano, and D. H. Silberberg. 1991. Galactosyl ceramide or a derivative is an essential component of the neural receptor for human immunodeficiency virus type 1 envelope glycoprotein gp120. *Proc. Natl. Acad. Sci. USA.* 88:7131–7134.
17. Harouse, J. M., S. Bhat, S. L. Spitalnik, M. Laughlin, K. Stefano, et al. 1991. Inhibition of entry of HIV-1 in neural cell lines by antibodies against galactosyl ceramide. *Science.* 253:320–323.
18. Bunow, M. R. 1979. Two gel states of cerebrosides. Calorimetric and Raman spectroscopic evidence. *Biochim. Biophys. Acta.* 574:542–546.
19. Koynova, R., and M. Caffrey. 1995. Phases and phase transitions of the sphingolipids. *Biochim. Biophys. Acta.* 1255:213–236.
20. Maggio, B., T. Ariga, J. M. Sturtevant, and R. K. Yu. 1985. Thermotropic behavior of binary mixtures of dipalmitoylphosphatidylcholine and glycosphingolipids in aqueous dispersions. *Biochim. Biophys. Acta.* 818:1–12.
21. Saxena, K., R. I. Duclos, P. Zimmermann, R. R. Schmidt, and G. G. Shipley. 1999. Structure and properties of totally synthetic galacto- and gluco-cerebrosides. *J. Lipid Res.* 40:839–849.
22. Kulkarni, V. S., and R. E. Brown. 1998. Thermotropic behavior of galactosylceramides with cis-monoenoic fatty acyl chains. *Biochim. Biophys. Acta.* 1372:347–358.
23. Brown, R. E., W. H. Anderson, and V. S. Kulkarni. 1995. Macro-ripple phase formation in bilayers composed of galactosylceramide and phosphatidylcholine. *Biophys. J.* 68:1396–1405.
24. Ali, S., H. L. Brockman, and R. E. Brown. 1991. Structural determinants of miscibility in surface films of galactosylceramide and phosphatidylcholine: effect of unsaturation in the galactosylceramide acyl chain. *Biochemistry.* 30:11198–11205.
25. Ruocco, M. J., D. Atkinson, D. M. Small, R. P. Skarjune, E. Oldfield, et al. 1981. X-ray diffraction and calorimetric study of anhydrous and hydrated N-palmitoylgalactosylsphingosine (cerebroside). *Biochemistry.* 20:5957–5966.
26. Curatolo, W., and L. J. Neuringer. 1986. The effects of cerebrosides on model membrane shape. *J. Biol. Chem.* 261:17177–17182.
27. Kulkarni, K., D. S. Snyder, and T. J. McIntosh. 1999. Adhesion between cerebroside bilayers. *Biochemistry.* 38:15264–15271.
28. Kulkarni, V. S., W. H. Anderson, and R. E. Brown. 1995. Bilayer nanotubes and helical ribbons formed by hydrated galactosylceramides: acyl chain and headgroup effects. *Biophys. J.* 69:1976–1986.
29. Ruocco, M. J., G. G. Shipley, and E. Oldfield. 1983. Galactocerebroside-phospholipid interactions in bilayer membranes. *Biophys. J.* 43:91–101.
30. Blanchette, C. D., W. C. Lin, T. V. Ratto, and M. L. Longo. 2006. Galactosylceramide domain microstructure: impact of cholesterol and nucleation/growth conditions. *Biophys. J.* 90:4466–4478.
31. Lin, W. C., C. D. Blanchette, and M. L. Longo. 2007. Fluid-phase chain unsaturation controlling domain microstructure and phase in ternary lipid bilayers containing GalCer and cholesterol. *Biophys. J.* 92:2831–2841.
32. Fidorra, M., L. Duelund, C. Leidy, A. C. Simonsen, and L. A. Bagatolli. 2006. Absence of fluid-ordered/fluid-disordered phase coexistence in ceramide/POPC mixtures containing cholesterol. *Biophys. J.* 90:4437–4451.
33. Angelova, M. I., S. Soléau, P. Meléar, J. F. Fauco, and P. Bothorel. 1992. Preparation of giant vesicles by external AC fields. Kinetics and applications. *Prog. Colloid Polym. Sci.* 89:127–131.
34. Parasassi, T., E. Kranowska, L. A. Bagatolli, and E. Gratton. 1998. Laurdan and Prodan as polarity-sensitive fluorescent membrane probes. *J. Fluoresc.* 8:365–373.
35. Parasassi, T., G. De Stasio, A. d'Ubaldo, and E. Gratton. 1990. Phase fluctuation in phospholipid membranes revealed by Laurdan fluorescence. *Biophys. J.* 57:1179–1186.

36. Parasassi, T., G. De Stasio, G. Ravagnan, R. M. Rusch, and E. Gratton. 1991. Quantitation of lipid phases in phospholipid vesicles by the generalized polarization of Laurdan fluorescence. *Biophys. J.* 60:179–189.

37. Bagatolli, L. A. 2006. To see or not to see: lateral organization of biological membranes and fluorescence microscopy. *Biochim. Biophys. Acta.* 1758:1541–1556.

38. Heimburg, T., and D. Marsh. 1993. Investigation of secondary and tertiary structural changes of cytochrome c in complexes with anionic lipids using amide hydrogen exchange measurements: an FTIR study. *Biophys. J.* 65:2408–2417.

39. Bagatolli, L. A., and E. Gratton. 2000. A correlation between lipid domain shape and binary phospholipid mixture composition in free standing bilayers: A two-photon fluorescence microscopy study. *Biophys. J.* 79:434–447.

40. Bagatolli, L. A., and E. Gratton. 2000. Two photon fluorescence microscopy of coexisting lipid domains in giant unilamellar vesicles of binary phospholipid mixtures. *Biophys. J.* 78:290–305.

41. Parasassi, T., M. Di Stefano, M. Loiero, G. Ravagnan, and E. Gratton. 1994. Influence of cholesterol on phospholipid bilayers phase domains as detected by Laurdan fluorescence. *Biophys. J.* 66:120–132.

42. Curatolo, W., B. Sears, and L. J. Neuringer. 1985. A calorimetry and deuterium NMR study of mixed model membranes of 1-palmitoyl-2-oleylphosphatidylcholine and saturated phosphatidylcholines. *Biochim. Biophys. Acta.* 817:261–270.

43. Lee, A. 1978. Calculation of phase diagrams for non-ideal mixtures of lipids, and a possible non-random distribution of lipids in lipid mixtures in the liquid crystalline phase. *Biochim. Biophys. Acta.* 507:433–444.

44. Maulik, P. R., and G. G. Shipley. 1995. X-ray diffraction and calorimetric study of N-lignoceryl sphingomyelin membranes. *Biophys. J.* 69:1909–1916.

45. Reed, R. A., and G. G. Shipley. 1987. Structure and metastability of N-lignocerylgalactosylsphingosine (cerebroside) bilayers. *Biochim. Biophys. Acta.* 896:153–164.

46. Maggio, B. 1994. The surface behavior of glycosphingolipids in biomembranes: a new frontier of molecular ecology. *Prog. Biophys. Mol. Biol.* 62:55–117.

47. Dietrich, C., L. A. Bagatolli, Z. N. Volovyk, N. L. Thompson, M. Levi, et al. 2001. Lipid rafts reconstituted in model membranes. *Biophys. J.* 80:1417–1428.

48. Veatch, S. L., and S. L. Keller. 2005. Seeing spots: complex phase behavior in simple membranes. *Biochim. Biophys. Acta.* 1746:172–185.

49. Bunge, A., P. Muller, M. Stockl, A. Herrmann, and D. Huster. 2008. Characterization of the ternary mixture of sphingomyelin, POPC, and cholesterol: support for an inhomogeneous lipid distribution at high temperatures. *Biophys. J.* 94:2680–2690.

50. Lee, A. G. 1977. Lipid phase transitions and phase diagrams. II. Mixtures involving lipids. *Biochim. Biophys. Acta.* 472:285–344.

51. Keller, S. G., and M.H.M.. 1999. Stripe phases in lipid monolayers near a miscibility critical point. *Phys. Rev. Lett.* 82:1602–1605.

52. Ali, M. R., K. H. Cheng, and J. Huang. 2006. Ceramide drives cholesterol out of the ordered lipid bilayer phase into the crystal phase in 1-palmitoyl-2-oleoyl-sn-glycero-3-phosphocholine/cholesterol/ceramide ternary mixtures. *Biochemistry.* 45:12629–12638.

53. Megha, and E. London. 2004. Ceramide selectively displaces cholesterol from ordered lipid domains (rafts): implications for lipid raft structure and function. *J. Biol. Chem.* 279:9997–10004.

54. Huang, J., and G. W. Feigenson. 1999. A microscopic interaction model of maximum solubility of cholesterol in lipid bilayers. *Biophys. J.* 76:2142–2157.

55. de Almeida, R. F., A. Fedorov, and M. Prieto. 2003. Sphingomyelin/phosphatidylcholine/cholesterol phase diagram: boundaries and composition of lipid rafts. *Biophys. J.* 85:2406–2416.